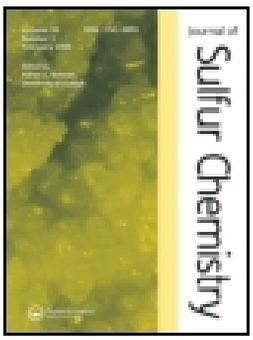

Journal of Sulfur Chemistry

ISSN: 1741-5993 (Print) 1741-6000 (Online) Journal homepage: http://www.tandfonline.com/loi/gsrp20

Crystal structure, computational studies, and stereoselectivity in the synthesis of 2-aryl-thiazolidine-4-carboxylic acids via in situ imine intermediate

Rohidas M. Jagtap, Masood A. Rizvi, Yuvraj B. Dangat & Satish K. Pardeshi

To cite this article: Rohidas M. Jagtap, Masood A. Rizvi, Yuvraj B. Dangat & Satish K. Pardeshi (2016): Crystal structure, computational studies, and stereoselectivity in the synthesis of 2-aryl-thiazolidine-4-carboxylic acids via in situ imine intermediate, Journal of Sulfur Chemistry, DOI: 10.1080/17415993.2016.1156116

To link to this article: http://dx.doi.org/10.1080/17415993.2016.1156116

JOURNAL OF SULFUR CHEMISTRY, 2016
http://dx.doi.org/10.1080/17415993.2016.1156116

Taylor & Francis
Taylor & Francis Group

Crystal structure, computational studies, and stereoselectivity in the synthesis of 2-aryl-thiazolidine-4-carboxylic acids via *in situ* imine intermediate

Rohidas M. Jagtap[a], Masood A. Rizvi[b], Yuvraj B. Dangat[c] and Satish K. Pardeshi[a]

[a]Department of Chemistry, Savitribai Phule Pune University (formerly University of Pune), Pune, India; [b]Department of Chemistry, University of Kashmir, Srinagar, India; [c]Physical Chemistry Division, CSIR-National Chemical Laboratory, Pune, India

ABSTRACT

This article presents the synthesis of (*2R/2S,4R*)-2-aryl-thiazolidine-4-carboxylic acids via nucleophilic addition of L-Cysteine on aromatic aldehydes involving a yield and time-effective room temperature reaction in an aqueous DMSO medium in the presence of $NaHCO_3$ as a base. The synthesized diastereomers were spectroscopically characterized and quantified for diastereomeric excess by liquid chromatography-mass spectrometry analysis. The impact of the type and position of substituent in aromatic aldehydes on reaction time, % yield, ^{1}H NMR shift at newly formed chiral center [C(2)-H], and diastereomeric excess (de%) have been investigated. A plausible mechanism for stereoselectivity via an *in situ* imine intermediate is proposed using real-time IR monitoring of the synthetic reaction based on the significant signals at 1597, 1593 cm^{-1} for imine (C = N) stretching. The imine mechanism for stereoselectivity was further supported by NMR studies of azomethine ^{13}C NMR signals at 159, 160 δ ppm and by the single crystal structure of hitherto unknown (*2S,4R*)-3-(tert-butoxycarbonyl)-2-(2-hydroxyphenyl)thiazolidine-4-carboxylic acid **(3a)** obtained as a major diastereomer in the synthesis of the butyloxy carbonyl (BOC) derivative of (*2R/2S,4R*)-2-(2-hydroxyphenyl)thiazolidine-4-carboxylic acid. The significant *ortho*-OH effect of phenolic hydroxyl group leading to strong hydrogen bondings plays a vital role in the formation of *2S,4R* BOC derivative stereoselectively. The frontier molecular orbitals, possible electronic excitations, IR band characterizations, and reactivity parameters of newly reported compound (**3a**) have been predicted using quantum chemical descriptors from density functional theory. The theoretical exploration of experimental spectra using time-dependent DFT indicated a ($\pi - \pi^*$) transition between HOMO and LUMO in the ultraviolet region.

ARTICLE HISTORY
Received 22 May 2014
Accepted 16 February 2016

KEYWORDS
2-aryl-thiazolidine-4-carboxylic acids; imine intermediate; X-ray crystal structure; density function theory; frontier molecular orbitals

CONTACT Satish K. Pardeshi skpar@chem.unipune.ac.in

Supplemental data for this article can be accessed here. http://dx.doi.org/10.1080/17415993.2016.1156116

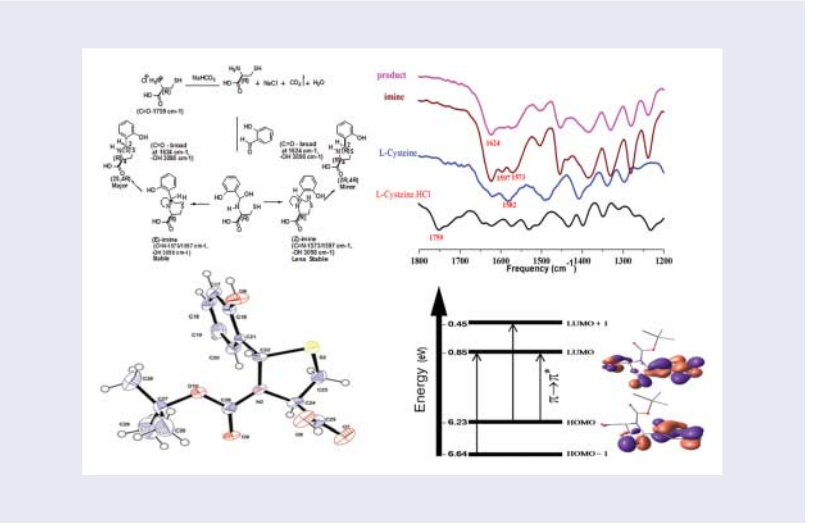

1. Introduction

Researchers have focused on organosulfur compounds because of their huge biological activities. Among these, thiazolidines have been revealed as a promising organosulfur class with a wide range of medicinal values.[1–9] Thiazolidine moieties have also been used as chiral heterocyclic ligands for transition metals and the crystal structures of some mononuclear nickel, cobalt complexes have been reported.[10] Recently 2D, 3D-QSAR and pharmacophore studies on thiazolidine-4-carboxylic acid derivatives as neuraminidase inhibitors in H_3N_2 influenza virus have also been reported.[11] Considering the importance of this class (thiazolidines) of compounds, studies comparing substituent-dependent reactivity of substrates and reagent specificity for their synthesis have been conducted.[12] The (*2R/2S,4R*)-2-aryl-thiazolidine-4-carboxylic acid (**2A-T4CA**) moieties have been synthesized from L-Cysteine hydrochloride by deploying several synthetic methods using a variety of bases and solvents such as AcOK-EtOH,[13] AcONa-EtOH,[14] AcOK-EtOH-Benzene,[15] NaOH-EtOH,[16] NaOH-H_2O-Dioxane,[17] Et_3N-EtOH,[18] Et_3N-NMP,[19] $TiCl_4$-EtOH-NaOH,[20] $NaHCO_3$-EtOH[04], Pyridine-H_2O.[21] The natural *4R* stereo center in 2A-T4CA can be also utilized to enhance stereoselectivity in L-proline-based organo-catalytic synthesis.[22] In spite of the variety of synthetic methods for thiazolidines, better protocols using non-volatile media, simple reagents, and time-efficient reactions to give high-purity products is always desired. Besides, none of the synthetic reports, mentioned above, focus on stereoselectivity of the products. In cognizance with the concept of asymmetric induction, correlating impact of the stereochemistry of groups present in a substrate with the control of chiral purity in the product, we report the synthesis of **2A-T4CA** through room temperature reaction in water-DMSO medium in presence of $NaHCO_3$ as a base. The complete characterization of diastereomeric products and stereoselectivity in terms of diastereomeric excess (de %) is reported. The impact of aromatic aldehyde substituent on reaction time, and % yield is also reported. Real-time IR and NMR monitoring of the reaction and the crystal structure of the unknown (*2S,4R*)-3-(tert-butoxycarbonyl)-2-(2-hydroxyphenyl)thiazolidine-4-carboxylic acid (**3a**)

are used to propose an imine intermediate mechanism. The physicochemical properties of this newly reported major diastereomer (**3a**) have been computationally explored with density functional theory (DFT) at the recommended CAM-B3LYP/6-311G + (*d*,*p*) level using Gaussian 09 software and compared with experimentally obtained values.

2. Results and discussion

2.1. Synthesis of (2R/2S,4R)-phenylthiazolidine-4 -carboxylic acid (2a) and role of solvent

The synthesis of (*2R/2S,4R*)-phenylthiazolidine-*4*-carboxylic acid from L-Cysteine hydrochloride and Benzaldehyde was used as a model reaction (Scheme 1, R=H) for solvent optimization of **2A-T4CA** synthesis in different solvents using equimolar quantities of substrate and reagents. The optimization results for compound **2a** are shown in Table 1.

Among the ten solvents studied (Table 1), 20% aqueous DMSO was found optimum for the synthesis of (**2a)** in terms of percent yield and reaction time, which is attributed to appropriate polarity of the medium suitable for solubility and reactivity of the components of the reaction. Furthermore, increasing water content after completion of reaction in 20% aqueous DMSO resulted in product precipitation with excellent yields. Subsequent to optimizing the reaction medium, the scope of $NaHCO_3$ as a base in 20% aq. DMSO was explored for several other aromatic aldehydes with different substituents at variable positions on the aromatic ring (Scheme 1). The nucleophilic addition underwent smoothly to afford the respective diastereomers of **2A-T4CA** with fair purity and yields (Table 2, Entries 1–18).

2.2. Setereochemical analysis and impact of substituents in synthesis

The presence of diastereomers was reflected in the signal replication pattern in ^{1}H and ^{13}C NMR spectra of **2A-T4CA**, showing difference in chemical shifts as well as coupling constants for similarly positioned protons. The diastereomers were quantified by

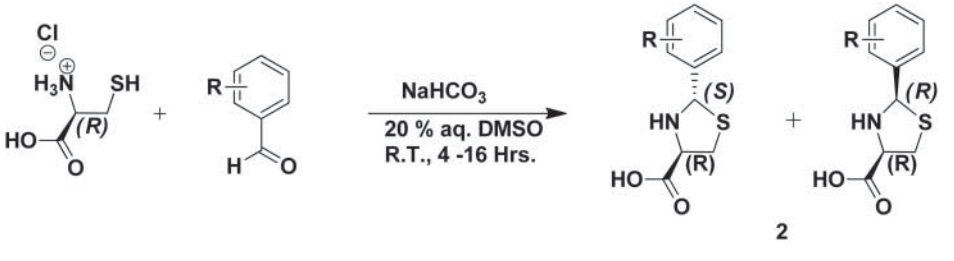

Scheme 1. Synthesis of 2A-T4CA.

Table 1. Optimization of the solvent medium for nucleophilic addition.

Entry	Solvent	Time (h)	Yield (%)	Entry	Solvent	Time (h)	Yield (%)
1	H_2O	26.0	86	6	50% aq. MeOH	13.0	91
2	Dioxane	18.0	83	7	DMSO	09.0	89
3	EtOH	14.0	87	8	10% aq. DMSO	10.5	92
4	MeOH	12.0	88	9	20% aq. DMSO	12.0	94
5	50% aq. EtOH	13.5	90	10	30% aq. DMSO	10.0	91

Table 2. Stereochemical impact of substituent on synthesis of 2A-T4CA.

Entry	*R*	Product	Yield[a] (%)	Reaction time[b] (h)	Chemical shift C(2)-H (δ ppm)[c]	de[d] (%)
1	H	2a	82	12.0	5.5, 5.7	00
2	2-OH	2b	78	12.5	5.7, 5.8	40
3	2-OCH_3	2c	83	14.0	5.5, 5.6	46
4	2-NO_2	2d	91	05.0	6.3, 6.9	68
5	3-NO_2	2e	80	12.0	5.7, 5.9	04
6	4-CH_3	2f	70	12.0	5.4, 5.5	00
7	4-OCH_3	2g	86	13.5	5.4, 5.5	10
8	4-Br	2h	73	14.0	5.5, 5.7	30
9	4-Cl	2i	73	13.5	5.5, 5.7	30
10	4-$N(CH_3)_2$	2j	62	18.0	5.1, 5.3	04
11	4-COOH	2k	88	09.0	5.6, 5.8	20
12	4-OH	2l	91	07.5	6.1, 6.3	30
13	2-OH, 4-OCH_3	2m	80	13.5	5.4, 5.6	64
14	2-OCH_3, 4-OH	2n	84	12.0	5.3, 5.5	76
15	3-OCH_3, 4-OH	2p	82	13.0	5.5,5.4	62
16	2,3-OH	2q	83	14.5	5.6, 5.8	60
17	3,4-OH	2r	75	11.0	5.3, 5.8	20
18	2,6-Cl	2s	85	12.0	6.2	98

[a]Overall yields.
[b]Obtained by TLC monitoring.
[c]Obtained from ^{1}H NMR spectra.
[d]Obtained from LCMS analysis using commercial column.

Liquid chromatography-mass spectrometry (LCMS) analysis of the products (Supplementary data, Figure S1). The stereochemical impact of different substituents and their positions was studied in terms of reaction time, % yield, chemical shift at newly generated chiral center [C(2)-H] and quantified by diastereomeric excess (de %), as shown in Table 2. It was observed that under our reaction conditions, the presence of electron-withdrawing groups such as -NO_2 reduced reaction time (5 h.), while electron-donating groups such as -OH (12.5 h.) and -OCH_3 (14 h.) increased reaction time in comparison to unsubstituted benzaldehyde (12 h.) (Table 2, Entry 1–4). In the case of aldehydes with substituents at position-2, the reactivity of 2-nitrobenzaldehyde was the highest. The substitution at position-3 of the aromatic ring does not have any significant impact on reactivity of the aldehyde. The substitution at position -4 gave the following trend of reaction time: -NO_2 < -COOH < -CH_3, < -OCH_3, -Cl, < -Br, < -NMe_2, which also indicated that electron-withdrawing groups at position-4 increase rate of reaction. In case of disubstituted aromatic aldehydes, the time required for completion of reaction was in the range of 11.0–14.5 h. The 2-OH containing disubstituted aldehyde (Table 2, Entry-13) reacts slower than 2-OCH_3 (Table 2, Entry-14) possibly due to presence of intra molecular hydrogen bonding. All the compounds **(2a–2s)** were obtained in good yields (> 70%) under optimized reaction conditions except, compound **2j** (Table 2, Entry-10; 62%). This can be attributed to strong + R effect of -NMe_2 group, which diminishes the electrophilicity of the aldehyde.

2.3. Substituent Effects on chemical shifts and diastereoselectivity

The diverse shielding and de-shielding effect of substituents on aromatic aldehydes generate different chemical shifts at C(2)-H. The overall trend in chemical shift (δ ppm) values in case of electron-withdrawing substituents was 2-NO_2 > 4-NO_2 > 2, 6-Cl > 3-NO_2 > 4-COOH. While in the case of electron-donating groups the trend

was 4-NMe_2 < 2-OCH_3, 4-OH < 3,4-OH < 2-OH, 2-OCH_3 < 4-Me < 4-OMe < 2-OMe < 4-Br = 4-Cl < 2-OH. The slight enhancement noted in δ ppm values in the case of 2-OH (Table 2, Entry 2) in comparison to 2-OCH_3 (Table 2, Entry 3) is likely due to a significant field effect. Among all substituents, the 2-NO_2 (Table 2, Entry 4) exhibited the strongest deshielding (6.3, 6.9 δ ppm) due to synergism of −R and field effect. While the 4-NMe_2 substituent (Table 2, Entry 10) exerts a strong shielding due to a + R effect (5.1, 5.3 δ ppm). From an LCMS analysis, it is found that the substituent positions are more vital to decide % de values than their electronegativity. The reaction of benzaldehyde gave both isomers of **2a** in nearly equal proportions but when we put substituents in the 2-position the selectivity increased with their size (2-OH < 2-OMe < 2-NO_2) to give high % de values. The 3-NO_2 in **2e** showed a minor role in selectivity. The % de values were higher especially among electron-withdrawing groups at position-4, strongly implicating their role in stabilization of reaction intermediates. The presence of electron-donating groups at position-4 however showed lower % de values. For disubstituted aldehydes, the highest de % was obtained with at least one of the substituent present at position-2 (Table 2, Entry 13, 14, 16, 18). Compound **2s** gave the highest % de value, suggesting that both 2, 6 positioned substituent have a strong impact on holding the intermediate in one of the stable conformations.

2.4. *Proposed* in situ *imine intermediates mechanism*

The stereoselectivity of the reaction can be explained on the basis of the plausible mechanism shown in Scheme 2. The reaction is proposed to proceed via diastereomeric *E* or

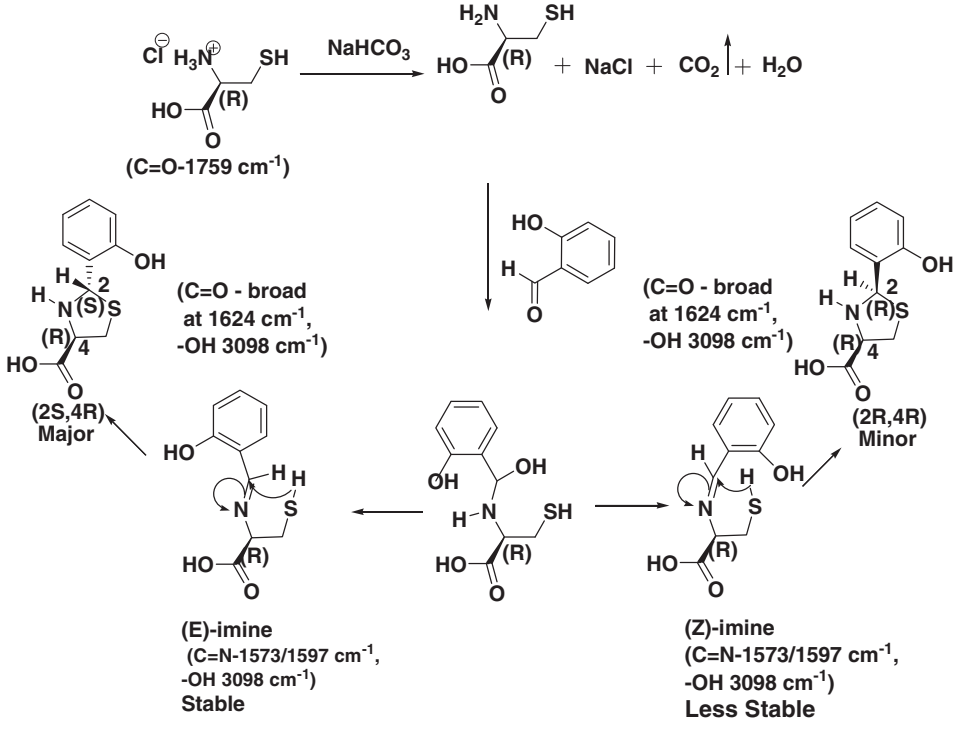

Scheme 2. Plausible mechanism with diastereomeric imines for synthesis of **2b**.

Z imine intermediates. The diastereomeric imines undergo cyclization by attack of thiol to give the corresponding diastereomers. The enhanced thermodynamic stability of the *E* isomer would result in the formation of *2S,4R* diastereomer as the major product.

The proposed imine intermediate mechanism is based on the real-time IR reaction monitoring for the synthesis of compound **2b**. To ascertain the existence of imines, the liquid fractions from reaction mixture (after addition of aldehyde) were quenched by ice at an every 10 min time intervals and monitored by IR spectroscopy to identify the −C = N stretching frequency peaks of imines (azomethines) as shown in Figure 1. In the course of reaction, the distinct, strongly hydrogen bonded −C = O stretching band at 1759 cm^{-1} in L-Cysteine hydrochloride disappeared due to generation of free amino acid by $NaHCO_3$ in aqueous DMSO medium. More concentration of zwitter ion and high nucleophilicity of S enable its initial attack on aldehyde, is not observed in this IR monitoring experiment, which supports the initial attack by amine nitrogen. The elimination of water from linear amino alcohols seems to be rapid as reflected in appearance of −C = N peaks in the fraction isolated at 10 min. The appearance of acid −C = O stretching at 1616 cm^{-1} along with two shoulder peaks at 1573 cm^{-1} and 1595 cm^{-1} attributed to −C = N stretching emerged and progressively became prominent upto 180 min. After completion of the reaction at about 12.5 h., the product showed broad distinct −C = O stretching signal at 1624 cm^{-1}, confirming that the imine intermediate has undergone cyclization to compound **2b.** This mechanism of stereoselectivity is in agreement with the proposed ring opening imine intermediate mechanism [23] for selective inversion at C_2 position in acetylation of Thiazolidine-4-carboxylic Acids. Recently the transformation of N-BOC T4CA (*2R/2S,4R*) diastereomers into single diastereomer (*2R,4R*) by dynamic kinetic resolution was proposed on the basis of imine (Schiff's base) intermediates.[24] Our work is of more

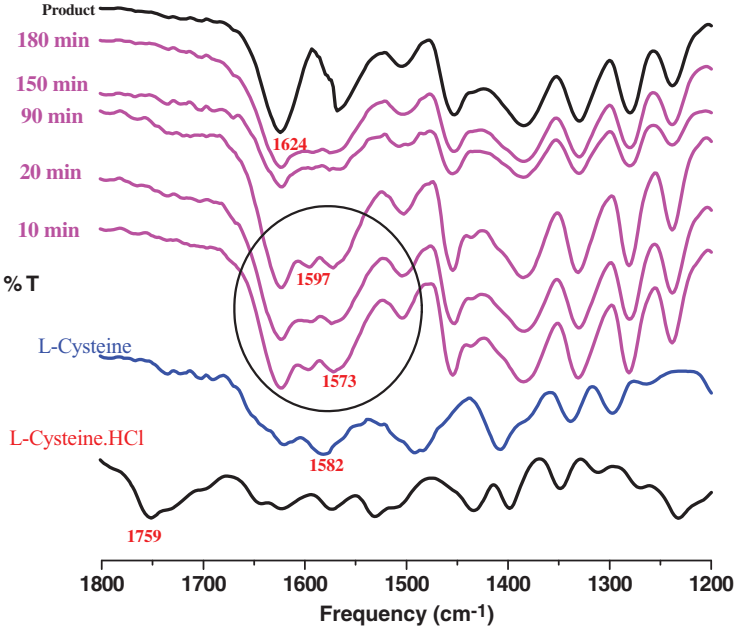

Figure 1. Real-time IR monitoring for synthesis of **2b**: investigation towards imine intermediates.

interest as it provides experimental support in favor of imine intermediate mechanism of diastereoselectivity in synthesis of 2-aryl-thiazolidine-4-carboxylic acids not reported so far.

Recently Ershov et al. [25] have reported the synthesis of 3-(3-mercapto-propionyl) thiazolidine-4-carboxylic acids and the ring-chain tautomerism of 2-aryl-6-oxohexahydro pyrimidine-4-carboxylic acid sodium salts in D_2O on the basis of NMR signals of linear azomethine intermediate.[26] In addition to real-time IR reaction monitoring, to ascertain the existence of linear imine, we have monitored the reaction by NMR spectroscopy to support the proposed mechanism for ring closure (Figure 2). The 0.2 mM (0.0350 g) of L-Cysteine HCl was dissolved in 0.6 ml of 20% DMSO-d_6 in D_2O in a NMR tube. The ^1H, ^{13}C NMR spectra of this clear sample solution were recorded. After recording the data, to the same tube 0.2 mM (0.0250 g) of Salicyldehyde was added and shaken for a minute. The resultant reaction mixture was immediately used to record ^1H NMR signals. From the ^1H NMR it is clear that, on addition of aldehyde the linear imine formation and its cyclization is rapid as H-5 singlet at 6.13, 6.34 δ ppm and azomethine proton signal at 9.19 δ ppm could be identified in only 3 -min scan. At 10 min scan for the CMR signals of reaction mixture, the appearance of signals at 159, 160 δ ppm represents azomethine carbons, whereas the minor signal at 62.63 δ ppm of C-4 carbon reveals the coexistence of linear imine and cyclized product **2b**. The $-\underline{C}H_2SH$ carbon signal still found at 36.27 δ ppm indicates the presence of unreacted amino acid. The minor downfield shifts in ^1H NMR signals for H-2 from 5.83, 5.64 δ ppm in pure **2b** to 6.13, 6.34 δ ppm in experimental spectra might be due the use of DMSO-d_6–D_2O solvent combination rather than only DMSO-d_6 used to record spectra of pure **2b**. These NMR studies strongly support the proposed linear imine intermediate mechanism.

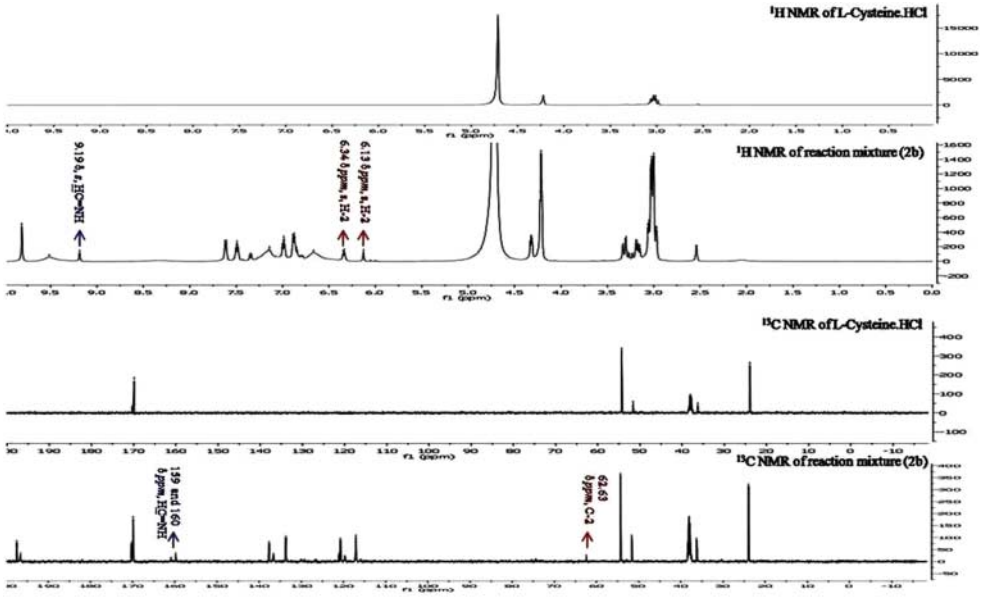

Figure 2. NMR studies for existence linear imine intermediate.

2.5. Confirmation of major diastereomer

Encouraged by the results, we decided to confirm the major diastereomer through unambiguous and definitive conformations in the crystal state using the X ray crystallography of the compound **2b** or its derivative which could corroborate to the understanding of stereochemical properties in solution. The tert-butoxycarbonyl (BOC) is known to be a wonderful protecting group; besides this, it can also build up a variety of weak intermolecular forces of attraction essential for packing of molecules during the crystal growth.[27] Visualizing this concept the compound **2b** was subjected for BOC protection of secondary amine. The reaction products got separated as solid diastereomeric mixture **3.** On solvent evaporation, purification and separation over the silica column it gave white solids **3a** with $[\alpha]_D^{25} + 10.7$ (*c* 1.25, MeOH) and **3b** with $[\alpha]_D^{25} + 73.2$ (*c* 1.25, MeOH), with individual yields 85% and 15%, respectively, as shown in Scheme 3. The $[\alpha]_D^{25}$ value of compound **3b** having *2R,4R* stereochemistry was in agreement with its structural analogs reported by Ershov et al.[25] The major product **3a** got crystallized by solvent diffusion method using $CHCl_3$-Hexane solvent system through slow evaporation of $CHCl_3$ solvent.

2.6. X-ray crystallographic structure of 3a

The compound **3a** is crystallized in monoclinic crystal system with $P2_1$ space group. A perspective view of compound **3a** through ORTEP diagram is shown in Figure 3 and the detailed crystallographic characteristics are summarized in supplementary data (Table S5). The asymmetric unit of **3a** contains two molecules with ortho −OH phenyl rings and functionalized thiazolidine rings oriented orthogonal to each other.

The C6–C7, C21–C22 bond lengths in compound **3a** are found as 1.501 Å, 1.503(1) Å, respectively. The torsion (dihedral) angles for S1–C7–C6–C1, N1–C7–C6–C5,

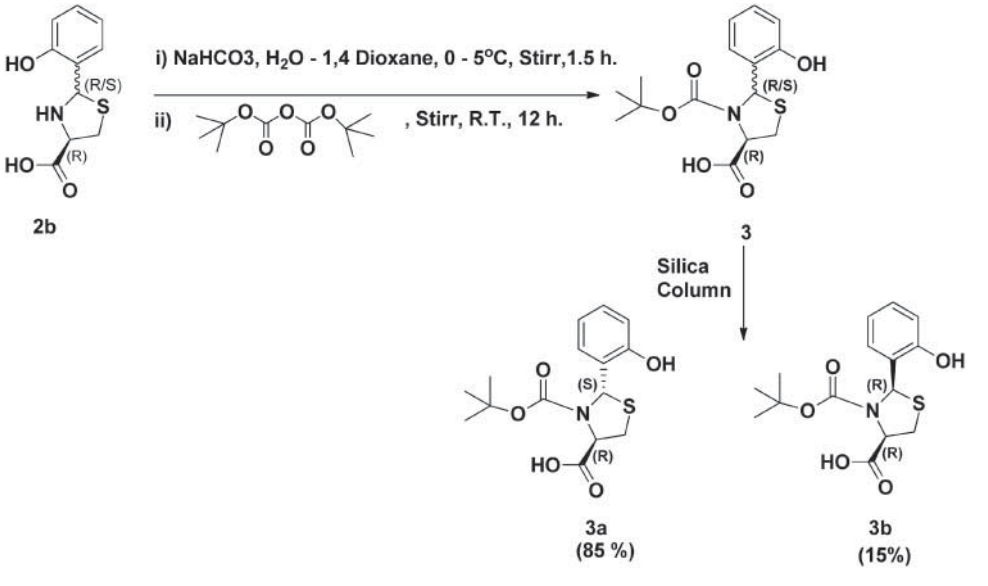

Scheme 3. Synthesis and separation of (*2R/2S,4R*)-3-(tert-butoxycarbonyl)-2-(2-hydroxyphenyl) thiazolidine-4-carboxylic acid.

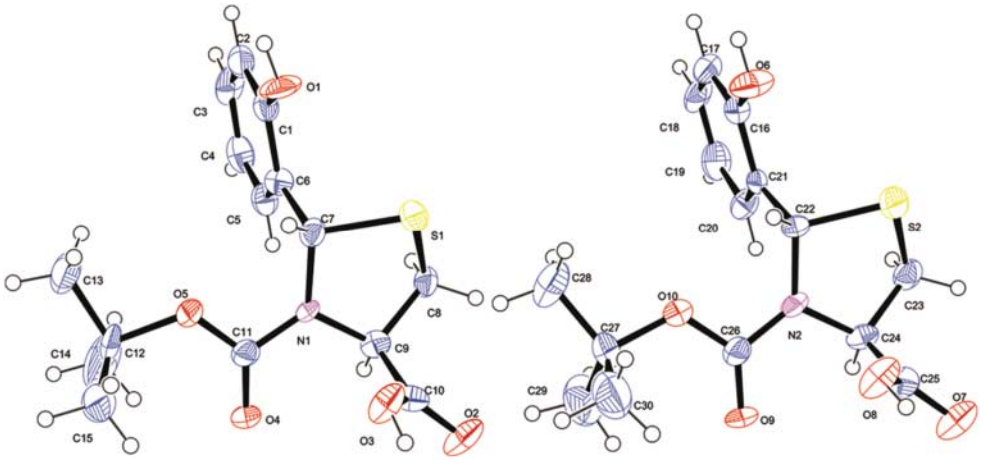

Figure 3. *ORTEP* view of the two molecules of compound (**3a**) in asymmetric unit with displacement ellipsoids drawn at 50%.

S2–C22–C21–C16 and N2–C22–C21–C20 are obtained as −77.31, −18.28°, −80.19° and −21.29°, respectively. The thiazolidine rings are functionalized with the carboxylic acid and N-BOC ester on adjacent atoms. The five-member thiazolidine rings are in slightly distorted cyclic conformation with S occupying *endo* position. The C8–S1 and C7–S1 bond length is 1.802(1) and 1.826(2) Å, respectively, along with C8-S1-C7 bond angle of 90.08(3)°. The X-ray structure of compound **3a** indicates the *2S, 4R* stereochemistry at the chiral carbons C7 and C9 in one molecule and same stereochemistry is maintained at C22, C24 of another molecule. The pendant carboxylic acid and carboxylate ester groups on the thiazolidine ring undergo extensive intermolecular hydrogen bonding, leading to the formation of a three-dimensional supramolecular assembly. Each molecule of **3a** shows four hydrogen bonding interactions with adjacent molecules, through two −OH group donors and two acceptor −C=O groups (Figure 4). The various hydrogen bond parameters of **3a** are given in Table 3. The supramolecular assembly of compound **3a** through hydrogen bonding interactions is shown in supplementary information (Figure S2).

Zhu et. al. [24] have recently reported the formation of exclusively single *2R,4R* similar N-BOC derivatives and their X-ray crystal structures having 2−Br, 2−OCH_3, 4−Cl substituents on aromatic ring The formation of major *2S,4R* diastereomer in our case distinguishes our work from this report. The preferred *2S* stereochemistry in **3a** may be attributed to significant ortho-OH effect in which phenolic hydrogen extends the strong H-bonding with carbonyl oxygen of carboxylate ester. This phenomenon may be playing a vital role to prefer the *2S, 4R* configuration in product, which ultimately results in the formation of **3a** as a major isomer.

2.7. DFT-optimized structure of 3a

DFT is a popular computational method of chemists for analysis of experimental properties. In this regard, we have performed DFT studies for perfect match of optimized structure with the experimental crystal structure. In this studies, for assigning transitions

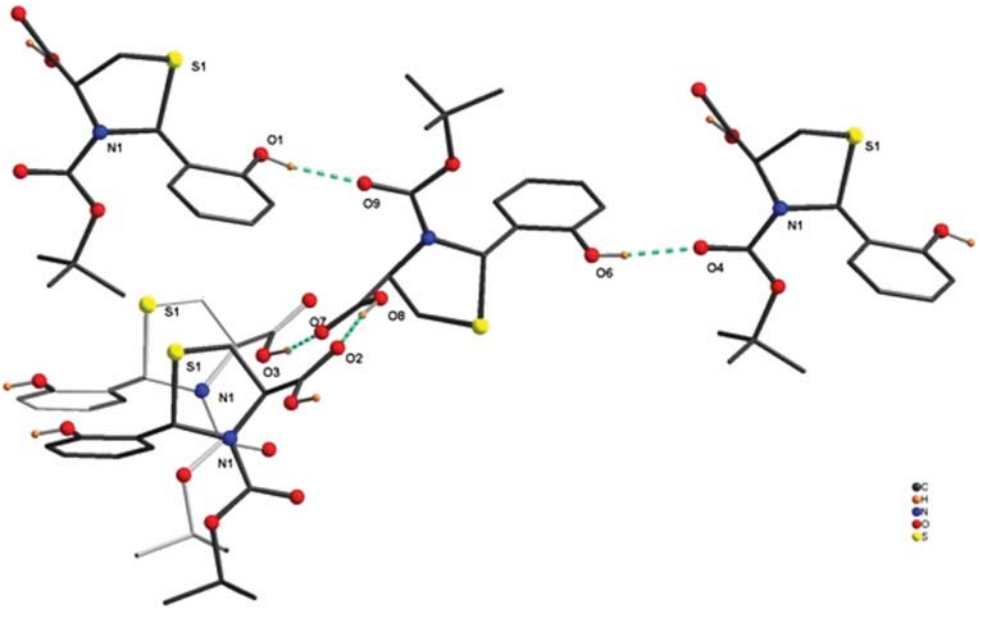

Figure 4. H-bonding pattern in **3a**.

Table 3. Hydrogen bond distance and angle for **3a** [Å and °].

D-H . . . A	d(D-H)	d(H . . . A)	d(D . . . A)	< (DHA)
O(1)-H(1A′) . . . O(9)#1	0.82	1.97	2.767 (6)	164.3
O(3)-H(3A′) . . . O(7)	0.82	1.93	2.665 (6)	149.0
O(6)-H(6A′) . . . O(4)#2	0.82	1.94	2.758 (6)	172.4
O(8)-H(8A′) . . . O(2)#3	0.82	1.87	2.674 (6)	164.3

Note: Symmetry transformations used to generate equivalent atoms: #1 $-x+1, y-1/2, -z+1$ #2 $-x+1, y+1/2, -z+2$ #3 $x-1, y, z$.

we used the recommended [28] Coulomb-attenuating method (CAM-B3LYP) in conjunction with polarizable continuum model of solvation (PCM) together with a 6-31G (d,p) basis set of DFT using Gaussian 09 software. The theoretical IR frequency bands assignment was done by considering the major fragments of molecule as thiazolidine ring, BOC ester, and hydroxyphenyl ring to generate theoretical IR spectra of compound **3a** (supplementary data, Table S6, Figure S3). Comparison of selected geometrical parameters of the X-ray crystallographic structure and DFT-optimized structure of the compound **3a** are depicted (supplementary data, Table S7) to produce the DFT-optimized theoretical crystal structure **(A)** as shown in Figure 5.

2.8. Optical behavior and stability of 3a

In order to explore any photovoltaic material property and to gain an insight of optical behavior of newly reported compound **3a** having two chiral centers, the absorption and emission spectra were recorded in three solvents as shown in Figure 6.

From Figure 6 it can be seen that the absorption and emission spectra of compound **3a** show a slight bathochromic shift with increasing solvent polarity. The experimental stokes

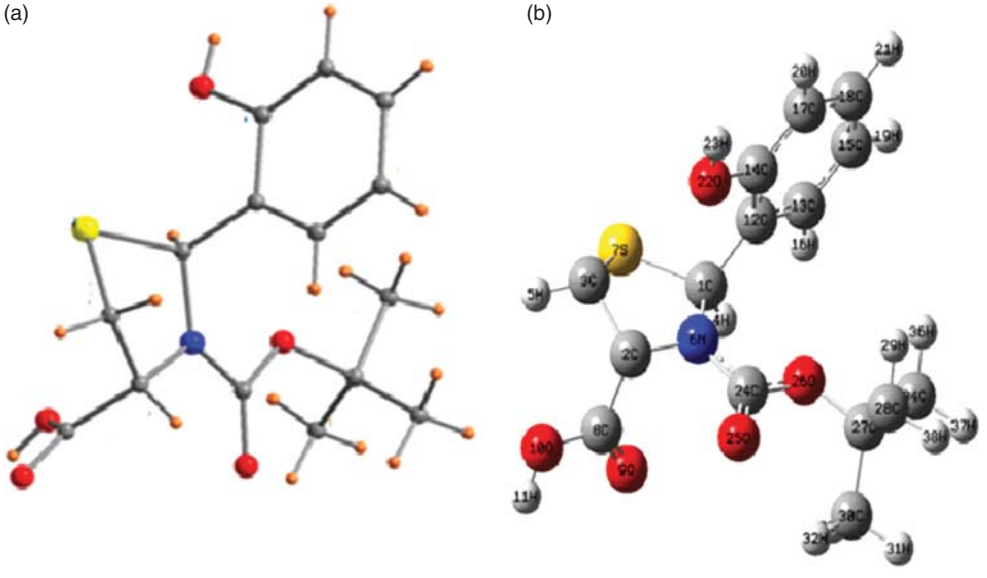

Figure 5. DFT-optimized (A) and X-ray crystallographic structure (B) of **3a**.

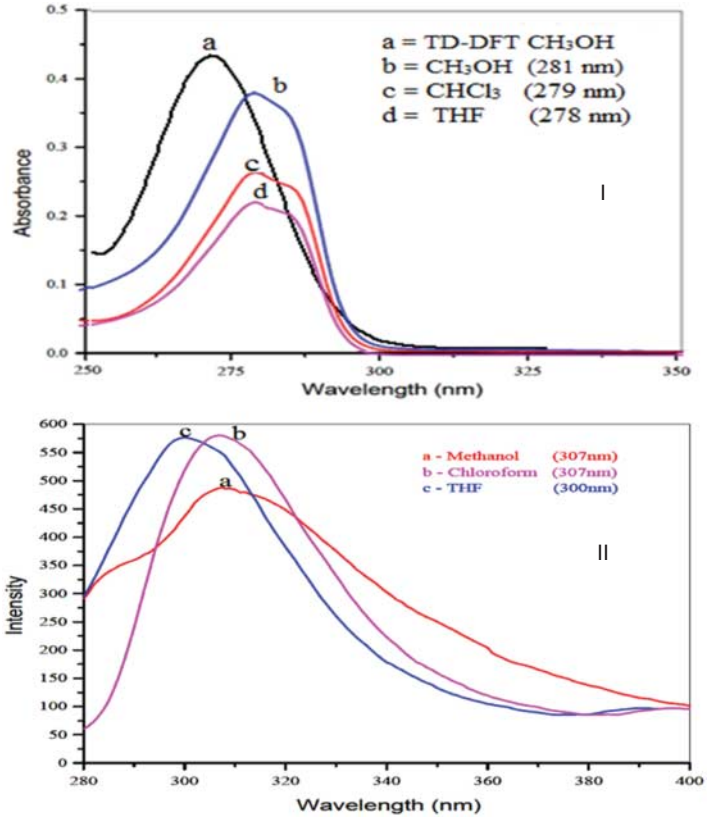

Figure 6. Absorption (I) and emission (II) spectra of compound **3a**.

shift (difference in absorption and emission maxima) was also found to be increasing with the increase in solvent polarity (26 and 22 nm respectively for methanol and THF). The lowered fluorescence intensity in case of methanol compared to chloroform and THF can be attributed to the solvent quenching.[29] In order to arrive at the nature of electronic transition in the case of compound **3a**, the HOMO–LUMO energies were computationally worked out from single point energy calculation of crystal structure of compound **3a** using CAM-B3LYP/6-31G (d,p) level of theory.[30] The computational analysis [31] revealed the absorption spectrum involving a ($\pi - \pi^*$) transition from HOMO to LUMO as possible electronic excitation in compound **3a**, which was also evident from the observed solvatochromic behavior.[32] The time-dependent density functional theory (TDDFT) calculation also indicate a ($\pi - \pi^*$) transition between HOMO and LUMO in ultraviolet region with an excitation energy of 4.60 eV corresponding to absorption wavelength of 269 nm(for $CHCl_3$ solvent), which is fairly close to its experimental value of 279 nm. The other theoretically possible transitions in ultraviolet region which are not experimentally distinct can be a HOMO-1 to LUMO and HOMO to LUMO + 1 transitions. A perspective view of frontier molecular orbitals of compound **3a** is shown in Figure 7.

The molecular orbital plots indicate that the electron density in case of HOMO is concentrated on sulfur atom and phenyl ring, while in the case of LUMO the electron density is predominantly on anti-bonding orbital of the phenyl ring. Quantum chemical descriptors are good to predict such properties of compound [33–35] and hence calculating such descriptors for a newly reported compound **3a** is interesting. The global reactivity descriptors such as electronegativity ($\chi = 3.54$ eV), hardness ($\eta = 5.38$ eV), and electrophillicity ($\omega = 1.16$ eV) of compound **3a** predict it to be a very stable compound, [36] which was also corroborated from molecular electrostatic potential plot in which the higher electron density is situated on more electronegative oxygen atoms (red) in comparison with very

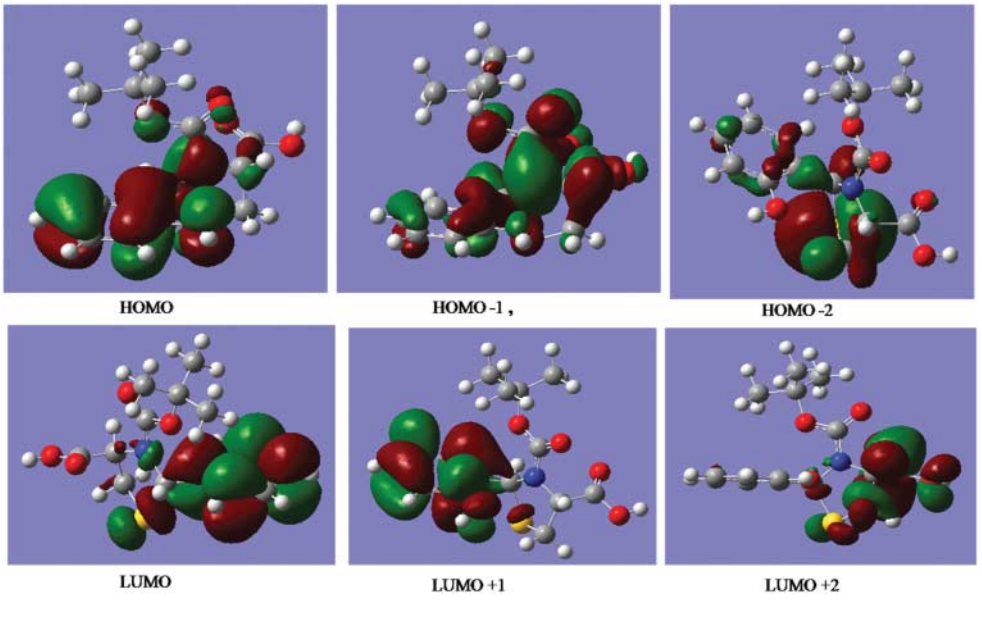

Figure 7. Frontier molecular orbitals of compound **3a**.

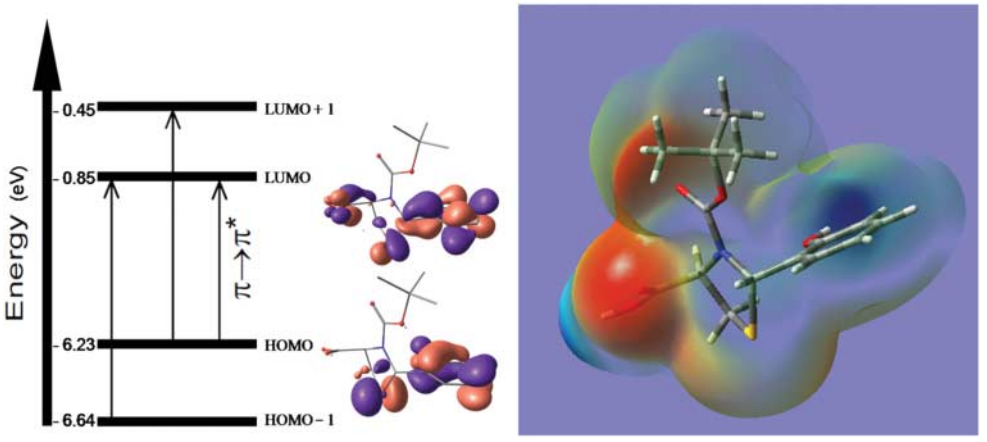

Figure 8. Electrostatic potential map and HOMO–LUMO orbital energy plots of compound **3a**.

lower electron density on less electronegative carbon and hydrogen atoms (blue) Figure 8. A band gap (HOMO–LUMO) of 5.38 eV, according to the frontier molecular orbital theory, may not easily lead to the formation of a transition state between the frontier orbitals of reactants.[37]

3. Conclusions

The present study demonstrated the efficient synthesis of **2A-T4CA** in 20% aqueous DMSO medium using $NaHCO_3$ as a base. The formation of **2A-T4CA** is proposed to occur via *in situ* imine intermediate in which *2S, 4R* diastereomer is the major isomer obtained from *E* imine and *2R, 4R* minor isomer obtained from *Z* imine. The plausible mechanism is supported by real-time IR profiling of the reaction and NMR studies. The X-ray single crystal structure of the N-BOC derivative **3a** further validates the possibility of imine intermediate in the synthesis of **2A-T4CA** in 20% aqueous DMSO medium. The electron density plot and other reactivity descriptors obtained from DFT study of newly reported compound **3a** predict it to be fairly stable. The quantum chemical calculations of **3a** using TDDFT indicate a ($\pi - \pi^*$) transition between HOMO and LUMO in ultraviolet region.

4. Experimental

4.1. General information

The TLC monitoring was done on Merck DC precoated TLC plates with 0.25 mm Kieselgel 60 F_{254}. Visualization was done using 254 nm UV lamp. All purified products were characterized by ^1H and ^{13}C-NMR spectroscopy in δ ppm (300 and 500 MHz NMR, VARIAN Mercury), IR spectroscopy in cm^{-1} (FTIR-8400 spectrometer, SHIMADZU), and elemental analysis was done using VARIAN EL-II instrument. The LCMS analysis was done using Ultra Fast Mass Spectrometer (LCMS-8030, SHIMADZU) with Chiracel OD column and isobutane as an eluting solvent. Super Nova Dual source X-ray Diffractometer System (Agilent Technologies) equipped with a CCD area detector was used for X-ray crystal structure.

NMR mechanistic study was done by ^{1}H and ^{13}C-NMR spectroscopy in δ ppm (500 MHz NMR, SHIMADZU) and specific rotation were taken using JASCO - P1020 polarimeter.

4.2. Solvent optimization for synthesis of (2R/2S,4R)-2- phenyl thiazolidine-4-carboxylic acid (2a)

The 1.0 mM (0.175 g) of L-Cysteine hydrochloride(**1**), 1.0 mM (0.084 g) $NaHCO_3$ and 0.95 mM (0.100 g) Benzaldehyde was stirred at R.T. in 40 ml of various solvents (Table 1, entries 1–10) such as H_2O, Dioxane, EtOH, MeOH, aq. EtOH, aq. MeOH, DMSO and aqueous DMSO. After total consumption of aldehyde, the reaction (monitored by TLC) mixture was poured on crushed ice, and precipitated white solid product was filtered and dried to get the diastereomeric (*2R/2S,4R*)-2-phenyl thiazolidine-4-carboxylic acid (**2a**).

4.3. Real-time IR monitoring for synthesis of (2R/2S,4R)-2-(2-hydroxyphenyl) thiazolidine-4-carboxylic acid (2b)

Initially the FT-IR spectrum for solid L-Cysteine hydrochloride was recorded as neat and the same instrument as well as program was used to record subsequent spectra. For real-time IR monitoring of the reaction, 1.0 mM (0.175 g) of L-Cysteine hydrochloride (**1**) and 1.0 mM (0.084 g) $NaHCO_3$ was stirred in 40 ml of 25% aq. DMSO at R.T. to a homogenous solution. After getting a clear solution, 0.25 ml solution fraction was collected, quenched in ice (about 2–3 g), and filtered under vacuum to dryness using Whatmann 42 paper to get a white solid examined for IR spectra of free amino acid (L-Cysteine). The zero time was set while addition 0.95 mM (0.122 g) Salicylaldehyde and the sample fractions from stirring reaction mixture were prepared by the above procedure and were monitored by IR spectroscopy at an interval of 10 min up to 180 min. The final IR spectrum represents the product precipitated at 12.5 h. as **2b**.

4.4. Synthesis and separation of (2R/2S,4R)-3-(tert-butoxycarbonyl)-2-(2-hydroxyphenyl) thiazolidine-4-carboxylic acid (3)

The 1.0 mM (0.225) of **2b** and 2.5 mM (0.21 g) $NaHCO_3$ were taken in a 100 ml two neck flask and stirred in 25 ml 50% aqueous 1,4-dioxane at 0°C for 1.5 h., and 1.4 mM (0.305 g) of di-t-butyloxy carbonyl was added to it drop wise, continuously stirred by natural heating to R.T. for 12 h. The reaction mixture was acidified up to pH 4.0 by cold 2N HCl and extracted in ethyl acetate. The extract was washed by cold saturated $NaHCO_3$ and the aqueous layer acidified up to pH 4.0 by cold 2N HCl. The acidic medium solution was extracted in DCM, which on solvent evaporation gave an oily solid **3**. The mixture **3** on purification and separation by silica column chromatography using 40% ethyl acetate in hexane gave white solids **3a** (*2S,4R* diastereomer) and **3b** (*2R,4R* diastereomer) with isolated yields 85% and 15%, respectively.

4.5. Crystal structure determination of 3a and refinement

Single crystals of compound **3a** were directly obtained by room temperature evaporation of $CHCl_3$ solution of reaction product purified from silica column. A colorless single

crystal (0.38×0.18×0.06 mm) of $C_{15}H_{19}N_1O_5S_1$ was placed in 0.7 mm diameter nylon CryoLoops (Hampton Research) with Paraton-N (Hampton Research). The loop was mounted on a Super Nova Dual source X-ray Diffractometer system (Agilent Technologies) equipped with a CCD area detector and operated at 250 W power (50 kV, 0.8 mA) to generate Mo Kα radiation ($\lambda = 0.71073$ Å) at 296(2) K. A total of 11580 reflections were collected of which 4721 were unique. The range of θ was from 6.06 to 58.22°. Data integration and indexing was carried out using Crystal clear, and structures were solved using direct method SIR-92. The complete refinement calculations were carried using programs in WinGX module. The final refinement of structures was carried out using full least square methods on F2 using SHELXL-97. The structure was solved in $P2_1$ space group, with $Z = 4$. All non-hydrogen atoms were refined anisotropically with hydrogen atoms generated as spheres riding the coordinates of their parent atoms. Final full matrix least-squares refinement on F^2 converged to $R_1 = 0.0867$ [I > 2σ (I)] and w$R_2 = 0.1924$ (all data) with GOF = 1.155.

4.6. Quantum chemical calculations

The DFT calculations performed in this work have been aimed to envisage the stability of synthesized compound **3a** through quantum chemical descriptors such as Frontier molecular orbitals (FMO), HOMO–LUMO energy gap, and reactivity parameters such as electronegativity, chemical hardness, electrophilicity index, and polarazability are depicted as electrostatic potential map. Besides assigning the experimental IR bands and exploring any possible photovoltaic material property, the TD-DFT calculations were performed in solvent (methanol) to gain insight into the electronic states giving rise to the absorption spectra. During TD-DFT calculations, the 10 lowest singlet–singlet transitions were considered. For the perfect match of optimized structure with the experimental crystal structure and more importantly for assigning transitions, we used the recommended Coulomb-attenuating method (CAM-B3LYP) in conjunction with PCM together with a 6-31G (d,p) basis set of DFT using Gaussian 09 software. In an MO framework, the chemical reactivity can be compared or predicted in terms of Global reactivity parameters such as electronegativity, chemical hardness and electrophilicity index.

4.6.1. Electronegativity

In Mullikan sense, electronegativity has been defined as the negative of the electronic chemical potential

$$\chi = -\mu\left(\frac{\partial E}{\partial N}\right)_{V(r)} = -\frac{I+A}{2} \tag{1}$$

where χ is electronegativity, μ is chemical potential, E is the total electronic energy, N is the no. of electrons, and $V(r)$ is the external electrostatic potential an electron feels at r due to the nuclei. Within the limitations of Koopmans' theorem, the orbital energies of the frontier orbitals are given by: $-E_{\mathrm{HOMO}} = I$; $-E_{\mathrm{LUMO}} = A$.

A very simple operational formula for μ, in terms of the one electron energies of HOMO and LUMO, ϵ_{H} and ϵ_{L}, is given by [38]

$$\mu \approx \frac{\varepsilon_H + \varepsilon_L}{2}. \tag{2}$$

4.6.2. Chemical hardness

The chemical hardness defines the resistance of the species to use electrons. The chemical hardness was calculated using the equation [39]

$$\eta \approx E_{\mathrm{LUMO}} - E_{\mathrm{HOMO}}. \tag{3}$$

4.6.3. Electrophilicity index

The electrophilicity index tells us about the strength of electrophilicity of the species and is calculated as [40]

$$\omega = \frac{\mu^2}{2\eta}. \tag{4}$$

The electrophilicity index given in Eq. (4) encompasses both the propensity of the electrophile to acquire an additional electronic charge driven by μ^2 and the resistance of the system to exchange electronic charge with the environment described by η simultaneously.

5. Physical and spectral data

5.1. (2R/2S,4R)-2- phenyl thiazolidine-4-carboxylic acid (2a)

White solid; yield: 0.17 g (82%). IR (KBr,υ,cm^{-1}): 3431(COOH), 1577(C = O), 1435(aromatic C-C), 1381(C-S), 1305(C-N), 1236(C-O), 1024, 895, 808 (aromatic C-H) cm^{-1}. ^{1}H NMR (300 MHz, DMSO-d_6): δ = 7.35–7.50 (m, 5H, J = 8, 2 Hz, H-Ar), δ = 7.20–7.33 (m, 5H, J = 8, 2 Hz, H-Ar), δ = 5.64 (s, 1H, H-2), δ = 5.47 (s, 1H, H-2), δ = 4.22 (t, 1H, J = 6.9, H-4), δ = 3.90 (t, 1H, J = 7 Hz, H-4), δ = 3.39–3.31 (m, 2H, J = 6.9, 4.5 Hz, H-5), δ = 3.25–3.01 (m, 2H, J = 7, 4.7 Hz, H-5).^{13}C NMR (75 MHz, DMSO-d_6): 172.92(C = O), 172.24(C = O), 141.25, 138.88, 128.42, 128.23, 128.15, 127.49, 127.20, 126.85 (C Ar), 71.72(C-2), 71.02(C-2), 65.57(C-4), 64.91(C-4), 38.98(C-5), 38.50(C-5). GCMS (APCI): 210.0 ($M^+ + 1$), 210.0 ($M^+ + 1$). Anal. calcd for $C_{10}H_{11}NO_2S$: C, 57.39; H, 5.30; N, 6.69; S, 15.32%. Found: C, 57.34; H, 5.32; N, 6.76; S, 15.28%.

5.2. (2R/2S,4R)-2-(2-hydroxyphenyl) thiazolidine-4-carboxylic acid (2b)

White solid; yield: 0.17 g (78%). IR (KBr,υ,cm^{-1}): 3097(COOH), 3010(N-H), 1627(C = O), 1383(C-S), 1332(C-N), 1280(C-O), 1238(C-O), 1097, 1093, 761 (aromatic C-H) cm^{-1}. ^{1}H NMR (300 MHz, DMSO-d_6): δ = 7.10–7.33 (m, 4H, J = 8, 2 Hz, H-Ar), δ = 6.73–6.82 (m, 4H, J = 8, 2 Hz, H-Ar), δ = 5.83 (s, 1H, H-2), δ = 5.64 (s, 1H, H-2), δ = 4.21 (t, 1H, J = 6 Hz, H-4), δ = 3.83 (t, 1H, J = 8 Hz, H-4), δ = 3.4 (q, 2H, J = 8 Hz, H-5), δ = 3.33 (q, 1H, J = 8 Hz, H-5).

^{13}C NMR (75 MHz, DMSO-d_6): 172.92(C = O), 172.24(C = O), 155.13, 154.54, 128.99, 128.60, 127.84, 127.49, 126.04, 124.14, 118.99, 118.70, 115.62, 115.00(C Ar), 67.62(C-2), 65.54(C-2), 65.13(C-4), 64.72(C-4), 38.00(C-5), 36.00(C-5). GCMS (APCI): 226.00 ($M^+ + 1$), 226.00 ($M^+ + 1$). Anal. calcd for $C_{10}H_{11}NO_3S$: C, 53.32; H, 4.92; N, 6.22; S, 14.23%.Found: C, 53.39; H, 4.92; N, 6. 35; S, 14.25%.

5.3. (2R/2S,4R)-2-(2-methoxyphenyl) thiazolidine-4-carboxylic acid (2c)

White solid; yield: 0.19 g (83%). IR (KBr,υ,cm^{-1}): 3500(broad) 1642(C=O), 1490(aromatic C-C), 1334(C-N), 1244(C-O) cm^{-1}.^{1}H NMR (300 MHz, DMSO-d_6): δ = 7.51–7.20 (m, 4H, J = 8, 2 Hz, H-Ar), δ = 7.05–6.85 (m, 4H, J = 8, 2 Hz, H-Ar), δ = 5.82 (s, 1H, H-2), δ = 5.62 (s, 1H, H-2), δ = 4.22 (t, 1H, J = 6 Hz, H-4), δ = 3.86 (t,1H, J = 3, 8 Hz, H-4), δ = 3.82 (s, 3H, H CH_3), δ = 3.72 (s, 3H, H CH_3), δ = 3.18–3.05 (m, 2H, J = 6 Hz, H-5), δ = 3.04–2.85(m, 2H, J = 8,3 Hz H-5).

^{13}C NMR (75 MHz, DMSO-d_6): 172.75(C=O), 172.24(C=O), 156.5, 156.1, 130.1, 129.2, 128.1, 127.2, 126.4, 125.2, 120.4, 120.1, 111.2, 110.70 (C Ar), 66.20 (C-2), 65.30 (C-2), 64.98(C-4), 64.91(C-4), 55.43(C CH_3), 55.39(C CH_3), 37.50(C-5), 37.81(C-5). GCMS (APCI): 239.90 ($M^+ + 1$), 239.90 ($M^+ + 1$). Anal calcd for $C_{11}H_{13}NO_3S$: C, 55.21; H, 5.48; N, 5.85; S, 13.40%. Found: C, 55.18; H, 4.64; N, 5.80; S, 13.36%. $C_{11}H_{13}NO_3S$: C, 55.21; H, 5.48; N, 5.85; S, 13.40%. Found: C, 55.18; H, 4.64; N, 5.80; S, 13.36%.

5.4. (2R/2S,4R)-2-(2-nitrophenyl) thiazolidine-4-carboxylic acid (2d)

Yellow solid; yield: 0.23 g (91%). IR (KBr,υ,cm^{-1}): 2797(broad, COOH), 1633(C=O), 1433(N-O), 1348(C-N), 1195(C-O) cm^{-1}.^{1}H NMR (300 MHz, DMSO-d_6): δ = 8.10–8.03 (m, 2H, J = 8 Hz, H-Ar), δ = 7.97–7.91 (m, 2H, J = 10 Hz, H-Ar), δ = 7.85–7.81 (m, 2H, J = 8 Hz, H-Ar), δ = 7.76–7.66 (m, 2H, J = 8 Hz, H-Ar), δ = 6.76 (s, 1H, H-2), δ = 6.33 (s, 1H, H-2), δ = 4.02 (t, 1H, J = 7 Hz, H-4), δ = 3.19 (q, 1H, J = 7, 3 Hz, H-4), δ = 3.03 (m, 2H, J = 7, 5 Hz, H-5), δ = 2.72(m, 2H, J = 7, 3 Hz, H-5).

^{13}C NMR (100 MHz, DMSO-d_6): 172.97(C=O), 172.80(C=O), 148.80, 147.90, 139.22, 135.86, 134.22, 133.79, 129.59, 128.92, 127.85, 125.77, 124.65(C Ar), 66.77(C-2), 65.96(C-2), 65.67(C-4), 65.32(C-4), 37.31(C-5), 36.99(C-5). GCMS (APCI): 254.00 ($M^+ + 1$), 254.00 ($M^+ + 1$). Anal. calcd for $C_{10}H_{10}N_2O_4S$: C, 47.24; H, 3.96; N, 11.02; S, 12.61%. Found: C, 47.24; H, 4.01; N, 11.08; S, 12.66%.

5.5. (2R/2S,4R)-2-(3-nitrophenyl) thiazolidine-4-carboxylic acid (2e)

Yellow solid; yield: 0.20 g (80%). IR (KBr,υ,cm^{-1}): 3435 (broad, COOH), 3279(N-H), 1730(C=O), 1627(C=O), 1529(N-O), 1448(C-N), 1205(C-O), 1157, 835(aromatic C-H) cm^{-1}. ^{1}H NMR (300 MHz, DMSO-d_6): δ = 8.20 (dd, 2H J = 2 Hz, H-Ar), δ = 8.05 (m, 2H, J = 2,8 Hz, H-Ar), δ = 7.97 (dd, 2H, J = 8, 2 Hz, H-Ar), δ = 7.65 (dd, 2H, J = 8 Hz, H-Ar), δ = 5.86 (s,1H,H-2), δ = 5.68 (s,1H, H-2), δ = 4.14 (t, 1H, J = 9 Hz, H-4), δ = 3.93–3.98 (dd, 1H, J = 9, 3 Hz, H-4), δ = 3.36 (m, 2H, J = 9, 3 Hz, H-5), δ 3.12 (m, 2H, J = 9, 3 Hz, H-5).

^{13}C NMR (75 MHz, DMSO-d_6): 172.50(C=O), 171.80(C=O), 147.70, 147.60, 144.60, 141.9, 134.2, 133.70, 129.80, 122.90, 122.30, 122.10, 121.20, 111.00 (H Ar), 70.07(C-2), 69.40 (C-2), 65.80(C-4), 64.70(C-4), 38.08(C-5), 38.20(C-5), GCMS (APCI): 254.00 ($M^+ + 1$), 254.00 ($M^+ + 1$). Anal. calcd for $C_{10}H_{10}N_2O_4S$: C, 47.24; H, 3.96; N, 11.02; S, 12.61%. Found: C, 47.20; H, 3.99; N, 11.04; S, 12.65%.

5.6. (2R/2S,4R)-2-(4-methyl phenyl) thiazolidine-4-carboxylic acid (2f)

White solid; yield: 0.16 g (70%). IR (KBr,υ,cm^{-1}): 3431(broad, COOH), 1577(C=O), 1435(C-N), 1381(C-S), 1305(C-N), 1236(C-O), 1024, 922, 895, 808, 765, 696 (aromatic

C-H) cm^{-1}.^{1}H NMR (300 MHz, DMSO-d_6): δ = 7.35–7.50 (m, 4H, J = 2,8 Hz, H Ar), δ = 7.20–7.33 (m, 4H, J = 2,8 Hz, H Ar), δ = 5.64 (s, 1H, H-2), δ = 5.47 (s, 1H, H-2), δ = 4.22 (t, 1H, J = 6.9 Hz, H-4), δ = 3.90 (t, 1H, J = 7 Hz, H-4), δ = 3.39 (m, 2H, J = 7, 3 Hz, H-5), δ 3.25 (m,2H, J = 7, 3 Hz, H-4), 2.5 (s, 6H, H $2CH_3$).

^{13}C NMR (75 MHz, DMSO-d_6): 172.92(C=O), 172.24 (C9=O), 141.25, 138.88, 128.42, 128.23, 128.15, 127.49, 127.20, 126.85(C Ar), 71.72(C-2),71.02 (C-2), 65.57(C-4), 64.91(C-4), 38.98(C-5), 38.50 (C-5), 20.67 (C CH_3), 20.62 (C CH_3). GCMS (APCI): 224.00 ($M^+ + 1$), 224.00 ($M^+ + 1$). Anal. calcd for $C_{11}H_{13}NO_2S$: C, 59.17; H, 5.87; N, 6.27; S, 14.36%. Found: C, 59.12; H, 5.865; N, 6.268; S, 14.37%.

5.7. (2R/2S,4R)-2-(4-methoxyphenyl) thiazolidine-4-carboxylic acid (2g)

White solid; yield: 0.20 g (86%). IR (KBr,υ,cm^{-1}): 1797(C=O), 1579 (aromatic C=C), 1510(C-N), 1303 (C-S), 1204 (C-O), 1028, 835, 810 (aromatic CH) cm^{-1}. ^{1}H NMR (300 MHz, DMSO-d_6): δ = 7.4 (dd, 2H, J = 9 Hz, H Ar), δ = 6.90 (dd, 2H, J = 9 Hz, H Ar), δ = 5.59 (s, 1H, H-2), δ = 5.45 (s, 1H, H-2), δ = 4.26 (t, 1H, J = 7 Hz, H-4), δ = 4.10 (t, 1H, J = 7 Hz, H-4), δ = 3.75 (s, 3H, H CH_3), δ = 3.74 (s, 3H, H CH_3), δ = 3.47–3.35 (m, 2H, J = 7, 3 Hz, H-5), δ = 3.32–3.15 (m, 2H, J = 7,4 Hz, H-5).

^{13}C NMR (75 MHz, DMSO-d_6): 172.98(C=O), 172.18(C=O), 159.15, 158.69, 132.65, 130.56, 128.53, 128.26, 113.71, 113.51(C Ar), 71.45 (C-2), 70.87 (C-2), 65.31 (C-4), 64.75(C-4), 55.05 (C $2CH_3$), 38.45(C-5), 37.81(C-5). GCMS (APCI): 240.00 ($M^+ + 1$), 240.00 ($M^+ + 1$).Anal. calcd for $C_{11}H_{13}NO_3S$: C, 55.21; H, 5.48; N, 5.85; S, 13.40%. Found: C, 55.18; H, 5.51; N, 5.88; S, 13.42%.

5.8. (2R/2S,4R)-2-(4-bromophenyl) thiazolidine-4-carboxylic acid (2h)

Pale yellow; yield: 0.21 g (73%). IR (KBr,υ,cm^{-1}): 3431 (broad, COOH), 3014(N-H),1629 (C=O), 1491(C-N), 1375(C-S), 1257(C-N), 1288 (C-O), 1076, 1003, 875, 858, 823, 802 (aromatic C-H) cm^{-1}. ^{1}H NMR (300 MHz, DMSO-d_6): δ = 7.57–7.37 (m, 8H, J = 8, 2 Hz, H Ar), δ = 5.68 (s, 1H, H-2), δ = 5.48 (s, 1H, H-2), δ = 4.15 (t, 1H, J = 7 Hz, H-4), δ = 3.87 (t, 1H, J = 7 Hz, H-4), δ = 3.26–3.39 (m, 2H, J = 7, 3 Hz, H-5), δ = 2.82–2.98 (m, 2H, J = 7, 3 Hz, H-5).

^{13}C NMR (75 MHz, DMSO-d_6): 172.73(C=O), 171.98 (C=O), 141.15, 140.68, 138.57, 138.13, 132.58, 131.84, 131.25, 131.00, 129.51, 129.20, 129.05, 128.70 (C Ar), 70.70 (C-2), 70.03 (C-2), 65.57(C-4), 64.79 (C-4), 38.28 (C-5), 37.90 (C-5). GCMS (APCI): 289.85 ($M^+ + 1$), 289.85 ($M^+ + 1$).Anal. calcd for $C_{10}H_{10}BrNO_2S$: C, 41.68; H, 3.50; N, 4.86; S, 11.13%. Found: C, 41.64; H, 3.52; N, 4.82; S, 11.17%.

5.9. (2R/2S,4R)-2-(4-chlorophenyl) thiazolidine-4-carboxylic acid (2i)

White solid; yields: 0.18 g (73%). IR (KBr,υ,cm^{-1}): 2962 (COOH), 1583(C=O), 1489 (C-N), 1384(C-S), 1209(C-O), 1091, 1012, 862, 819 (aromatic C-H) cm^{-1}.^{1}H NMR (300 MHz, DMSO-d_6): δ = 7. 60–7.25 (m, 8H, J = 8, 2 Hz, H Ar), δ = 5.65 (s, 1H, H-2), δ = 5.45 (s, 1H, H-2), δ = 4.15 (t, 1H, J = 6 Hz, H-4), δ = 3.87 (t, 1H, J = 8 Hz, H-4), δ = 3.48 (s, broad, 1H, residual H_2O from solvent), δ = 3.39–3.26 (m, 2H, J = 6, 3 Hz, H-5), δ = 3.05–2.80 (m, 2H, J = 8, 3 Hz, H-5).

^{13}C NMR (75 MHz, DMSO-d_6): 172.79(C=O), 172.172.14(C=O), 140.82, 138.16, 132.58, 131.80, 129.17, 128.67, 128.35, 128.06, (C Ar), 70.78 (C-2), 70.03 (C-2), 65.80 (C-4), 64.91(C-4), 38.59 (C-5), 38.46 (C-5), GCMS (APCI): 243 ($M^+ + 1$), 243 ($M^+ + 1$). Anal. calcd for $C_{10}H_{10}ClNO_2S$:C, 49.28; H, 4.14; N, 5.75; S, 13.16%. Found: C, 49.32; H, 4.17; N, 5.72; S, 13.20%.

5.10. (2R/2S,4R)-2-(4-(dimethylamino)phenyl) thiazolidine-4-carboxylic acid (2j)

Pale brown solid; yields: 0.16 g (62%). IR (KBr,υ,cm^{-1}): 3029 (broad, COOH), 1614 (C=O), 1520(C=C), 1338 (C-S) cm^{-1}. ^{1}H NMR (300 MHz, DMSO-d_6): δ = 6.67 (d, 2H, J = 8 Hz, H Ar), δ = 7.25 (q, 2H, J = 7 Hz, H Ar), δ = 6.76 (d, 2H, J = 8 Hz, H Ar), δ = 6.66 (t, 2H, J = 8 Hz, H Ar), δ = 5.51 (s, 1H, H-2), δ = 5.38 (s, 1H, H-2), δ = 4.24 (dd, 1H, J = 5, 7 Hz, H-4), δ = 3.78–3.84 (t, 1H, J = 7 Hz, H-2), δ = 3.28–3.35 (m, 2H, J = 7, 5 Hz, H-5), δ = 3.14–3.25 (m, 2H, J = 7, 5 Hz, H-2), δ = 2.87(s,6H, H 2NC$\underline{H_3}$).

^{13}C NMR (75 MHz, DMSO-d_6): 172.90(C=O), 172.12(C=O), 159.11, 158.55, 132.25, 130.36, 128.44, 128.13, 113.06, 113.00(C Ar), 71.37 (C-2), 70.07 (C-2), 65.24 (C-4), 64.71(C-4), 40.03 (C 2N-$\underline{C}H_3$), 38.22(C-5), 37.41(C-5). GCMS (APCI): 252.90 ($M^+ + 1$), 252.90 ($M^+ + 1$). Anal. calcd for $C_{12}H_{16}N_2O_2S$:C, 57.12; H, 6.39; N, 11.10; S, 12.71%. Found: C, 57.14; H, 6.44; N, 11.08; S, 12.68%.

5.11. (2R/2S,4R)-2-(4-carboxyphenyl) thiazolidine-4-carboxylic acid (2k)

White solid; yields:0.22 g (88%). IR (KBr,υ,cm^{-1}): 3410 (COOH), 3228 (broad, N-H), 1710(C=O), 1629(C=O),1427(C=C), 1383(C-N), 1300(C-S), 1253(C-O) cm^{-1}. ^{1}H NMR (300 MHz, DMSO-d_6): δ = 7.93(d, 2H, J = 2, 8 Hz, H Ar), δ = 7.89 (d, 2H J = 9 Hz, H Ar), δ = 7.63(d, 2H, J = 8 Hz, H Ar), δ = 7.53 (d, 2H, J = 8 Hz, H Ar), δ = 5.77(s, 1H, H-2), δ = 5.58 (s,1H, H-2), δ = 4.17 (t, 1H, J = 6 Hz, H-4), δ = 3.92 (t, 1H, J = 9 Hz, H-4), δ = 3.31–3.27 (m, 2H, J = 6, 3 Hz, H-5), δ = 3.12–3.04 (dd, 2H, J = 9, 3 Hz, H-5).

^{13}C NMR (100 MHz, DMSO-d_6): 173.28 (C=O), 172.61 (C=O), 167.56 (C=O),167.48, 147.22, 147.46, 131.02, 130.62, 129.96, 129.82, 127.93, 127.39 (C Ar),71.43(C-2), 70.74 (C-2), 66.07 (C-4), 65.42 (C-4), 38.54(2C-5). GCMS (APCI): 253.95 ($M^+ + 1$), 253.95 ($M^+ + 1$). Anal. calcd for $C_{11}H_{11}NO_4S$: C, 52.16; H, 4.38; N, 5.53; S, 12.66%. Found: C, 52.20; H, 4.36; N, 5.55; S, 12.65%.

5.12. (2R/2S,4R)-2-(4-hydroxyphenyl) thiazolidine-4-carboxylic acid (2l)

White solid; yield 0.20 g (91%). IR (KBr,υ,cm^{-1}): 1797(C=O), 1579(C=C), 1510(C=C), 1020, 838, 813 (aromatic C-H) cm^{-1}. ^{1}H NMR (300 MHz, DMSO-d_6): δ = 7.38 (dd, 4H, J = 9 Hz), δ = 6.90 (dd, 4H, J = 9 Hz), δ = 5.57 (s, 1H), δ = 5.40 (s, 1H), δ 4.23 = (t, 1H, J = 7 Hz), δ 4.15 = (t, 1H, J = 7 Hz), δ = 3.45–3.33 (m, 2H, J = 7, 3 Hz),δ = 3.30–3.15 (m, 2H, J = 7, 4 Hz).

^{13}C NMR (75 MHz, DMSO-d_6): 172.08(C=O), 172.00(C=O), 159.05, 158.60, 132.62, 130.44, 128.03, 128.11, 113.61, 113.50 (C Ar), 71.40 (C-2), 70.27 (C-2), 65.26 (C-4), 64.65(C-4), 38.40(C-5), 37.51(C-5). GCMS (APCI): 225.95 ($M^+ + 1$), 225.95 ($M^+ + 1$).

Anal. calcd for $C_{10}H_{11}NO_3S$: C, 53.32; H, 4.92; N, 6.22; S, 14.23%. Found: C, 53.30; H, 4.87; N, 6. 26; S, 14.21%.

5.13. (2R/2S,4R)-2-(2-hydroxy-4-methoxyphenyl) thiazolidine-4-carboxylic acid (2m)

White solid; yield: 0.20 g (80%). IR (KBr,υ,cm^{-1}): 3304(broad, COOH), 3037(N-H), 1629(C = O), 1591, 1518(C = C), 1375(C-N), 1289(C-S), 1236(C-O), 1060, 1020, 977, 910, 824, 798 (aromatic C-H) cm^{-1}.^{1}H NMR (300 MHz, DMSO-d_6): δ = 6.94–6.8 (m, 6H, J = 8, 2 Hz, H Ar), δ = 5.51 (s, 1H, H-2), δ = 5.37 (s, 1H, H-2), δ = 4.22 (q, 1H, J = 6 Hz, H-4), δ = 3.85(dd, 1H, J = 6, 3 Hz, H-4), δ = 3.75 (s, 3H, H C$\underline{H}_3$), δ = 3.74 (s, 3H, H C$\underline{H}_3$), δ = 3.47–3.35 (m, 2H, J = 6, 3 Hz, H-5), δ = 3.15–3.32 (m, 2H, J = 8, 4 Hz, H-5).

^{13}C NMR (75 MHz, DMSO-d_6): 173.05(C = O), 172.37(C = O), 147.68, 147.18, 146.99, 133.24, 131.65, 124.40, 118.11, 117.78,114.35,114.27,113.45,111.87, (C Ar), 71.71(C-2), 71.07(C-2), 65.08(C-4), 64.73(C-4), 55.61 (C 2$\underline{C}H_3$), 38.42(C-5), 37.76(C-5). GCMS (APCI): 256.00 ($M^+ + 1$), 256.00 ($M^+ + 1$). Anal. calcd for $C_{11}H_{13}NO_3S$:C, 51.75; H, 5.13; N, 5.49; S, 12.56%. Found: C, 51.79; H, 5.11; N, 5.48; S, 12.52%.

5.14. (2R/2S,4R)-2-(2-methoxy-4-hydroxyphenyl) thiazolidine-4-carboxylic acid (2n)

White solid; yield 0.21 g (84%). IR (KBr,υ,cm^{-1}): 3452 (broad, COOH), 3111(N-H), 1614(C = O), 1516(C = C), 1381(C-N), 1244(C-O), 1051, 997, 831, 798 (aromatic C-H) cm^{-1}.^{1}H NMR (300 MHz, DMSO-d_6): δ = 7.26 (dd, 3H, J = 8 Hz, H Ar), δ = 6.73 (dd, 3H, J = 8, 2 Hz, H Ar), δ = 5.51 (s, 1H, H-2), δ = 5.37 (s, 1H, H-2), δ = 4.26(q, 1H, J = 6 Hz, H-4), δ = 3.91(t, 1H, J = 8 Hz, H-4), δ = 3.86 (s, 6H, H 2C$\underline{H}_3$), δ = 3.2–3.0 (m, 2H, J = 6, 4 Hz, H-5), δ = 3.2–3.0 (m, 2H, J = 8, 4 Hz, H-5).

^{13}C NMR (75 MHz, DMSO-d_6): 173.50(C = O), 172.86(C = O), 157.86, 157.37, 131.22, 129.28, 128.98, 128.77, 116.30, 115.62, 115.36 (C Ar), 74.30 (C-2), 71.67 (C-2), 65.81(C-4),65.22(C-4), 40.73(C $\underline{C}H_3$), 40.45(C $\underline{C}H_3$), 38.26(2C-5). GCMS (APCI): 256.00 ($M^+ + 1$), 256.00 ($M^+ + 1$). Anal calcd for $C_{11}H_{13}NO_3S$: C, 51.75; H, 5.13; N, 5.49; S, 12.56%. Found: C, 51.72; H, 5.18; N, 5.45; S, 12.58%.

5.15. (2R/2S,4R)-2-(2,3-dihydroxyphenyl) thiazolidine-4-carboxylic acid (2p)

White solid; yield: 0.20 g (82%). IR (KBr,υ,cm^{-1}): 3339(COOH), 3352(N-H), 1624(C = O), 1685(C = O), 1475, 1440(C = C), 1383(C-N), 1332(C-S), 1190(C-O) cm^{-1}.^{1}H NMR (300 MHz, DMSO-d_6): δ = 9.37 (broad s, 1H, H O$\underline{H}$), δ = 9. 25 (broad s, 1H, H O$\underline{H}$), δ = 6.71–6.79 (m, 3H, J = 8, 2 Hz, H Ar), δ = 6.55–6.68 (m, 3H, J = 7, 2 Hz, H Ar), δ = 5.83 (s, 1H, H-2), δ = 5.64 (s, 1H, H-2), δ = 4.21 (t, 1H, J = 6 Hz, H-4), δ = 3.82 (t, 1H, J = 8 Hz, H-4), δ = 3.36–3.30 (q, 2H, J = 6 Hz, H-5), δ = 3.05–2.96 (m, 2H, J = 8, 4 Hz, H-5).

^{13}C NMR (75 MHz, DMSO-d_6): 172.10(C = O), 172.00(C = O), 145.00, 144.00, 143.00, 124.00, 127.00, 124.00, 118.80, 118.50, 118.00, 116.60, 114.90, 114.30 (C Ar), 67.75(C-2), 65.80(C-2), 65.00(C-4), 64.75(C-4), 38.00(C-5), 36.50(C-5). GCMS (APCI): 241.95

($M^+ + 1$), 241.95 ($M^+ + 1$). Anal. calcd for $C_{10}H_{11}NO_4S$: C, 49.78; H, 4.60; N, 5.81; S, 13.29%. Found: C, 49.72; H, 4.61; N, 5.78; S, 13.28%.

5.16. (2R/2S,4R)-2-(3-methoxy-4-hydroxyphenyl) thiazolidine-4-carboxylic acid (2q)

White solid; yield: 0.21 g (83%). IR (KBr,υ,cm^{-1}): 3057 (broad), 1624(C=O), 1381(C-N), 1278(C-S), 1159(C-O), 1136, 1028, 844, 796(aromatic C-H) cm^{-1}.^{1}H NMR (300 MHz, DMSO-d_6): δ = 7.11 (d, 2H, J = 8 Hz, H Ar), δ = 7.03 (dd, 2H, J = 8 Hz, H Ar), δ = 6.90 (d, 2H, J = 2 Hz, H Ar), δ = 5.52 (s, 1H, H-2), δ = 5.39 (s, 1H, H-2), δ = 4.30 (dd, 1H, J = 7, 3 Hz, H-4), δ = 3.83 (q, 1H, J = 4, 7 Hz, H-4), δ = 3.76 (s, 3H, H C$\underline{H}_3$), δ = 3.75 (s, 3H, H C$\underline{H}_3$), δ = 3.25–3.36 (m, 2H, J = 7, 3 Hz, H-5), δ = 3.13–3.18 (m, 2H, J = 7, 4 Hz, H-5).

^{13}C NMR (75 MHz, DMSO-d_6):173.00(C=O), 172.72(C=O), 147.40, 14.30, 146.60, 146.20, 131.08, 129.20, 119.90, 119.60, 115.40, 115.10, 111.47, 111.28, (C Ar), 72.40 (C-2), 72.10 (C-2), 65.43(C-4), 64.70 (C-4), 55.60(C 2$\underline{C}H_3$), 38.37(C-5), 37.72(C-5). GCMS (APCI): 255.95 ($M^+ + 1$), 255.95 ($M^+ + 1$). Anal. calcd for $C_{11}H_{13}NO_3S$: C, 51.75; H, 5.13; N, 5.49; S, 12.56%. Found: C, 51.78; H, 5.13; N, 5.50; S, 12.53%.

5.17. (2R/2S,4R)-2-(3,4-dihydroxyphenyl) thiazolidine-4-carboxylic acid (2r)

White solid; yield: 1.8 g (75%). IR (KBr,υ,cm^{-1}): 3327(COOH), 3173(N-H), 1627(C=O), 1599(C=O), 1454(C-N), 1338(C-S), 1294(C-O), 1114, 1058, 829, 796(aromatic C-H) cm^{-1}.^{1}H NMR (300 MHz, DMSO-d_6): δ = 9.05 (broad s, 1H, H O$\underline{H}$), δ = 6.8 (m, 3H, J = 8, 2 Hz, H Ar), δ = 6.7 (m, 3H, J = 8, 2 Hz, H Ar), δ = 5.47 (s, 1H, H-2), δ = 5.32 (s, 1H, H-2), δ = 4.24 (t, 1H, J = 8 Hz, H-4), δ = 3.83 (t, 1H, J = 8 Hz, H-4), δ = 3.37–3.25 (m, 2H, J = 8, 4 Hz, H-5), 3.22–2.98 (m, 2H, J = 8, 4 Hz, H-5).

^{13}C NMR (75 MHz, DMSO-d_6):173.00(C=O), 172.30(C=O), 145.78, 145.20, 143.00, 144.93, 131.23, 131.17, 129.18, 118.26, 118.04, 115.43, 115.20, 114.69 (C Ar), 71.29 (C-2), 71.24 (C-2), 64.70(C-4), 65.04(C-4), 38.43(C-5), 37.64(C-5). GCMS (APCI): 241.95 ($M^+ + 1$), 241.95 ($M^+ + 1$). Anal. calcd for $C_{10}H_{11}NO_4S$: C, 49.78; H, 4.60; N, 5.81; S, 13.29%. Found: C, 49.79; H, 4.64; N, 5.80; S, 13.32.

5.18. (2R/2S,4R)-2-(2,6-dichlorophenyl) thiazolidine-4-carboxylic acid (2s)

White solid; yield: 0.23 g (85%). [α]D^{25}−101.1 (c 1.25, MeOH). IR (KBr,υ,cm^{-1}): 3454(COOH), 3298(N-H), 1726(C=O), 1330(C-S), 1271(C-O), 912, 781(aromatic C-H) cm^{-1}.

^{1}H NMR (300 MHz, DMSO-d_6): δ = 7.50 (dd, 1H, J = 8 Hz, H Ar), δ 7.42–7.37 (t, 2H, J = 7,2 Hz, H Ar), δ 6.42(s, 1H, H-2), δ 3.88 (dd, 1H, J = 10,6 Hz, H-4), δ 3.46 (dd, 1H, J = 10,6 Hz, H-5), δ 2.96 (t, 1H, J = 10 Hz, H-5).

^{13}C NMR (75 MHz, DMSO-d_6):173.00(C=O), 134.00, 131.00, 130.00, 129.00, 128.60, 128.00(C Ar), 70.00 (C-2), 63.41 (C-4), 38.58 (C-5). GCMS (APCI): 277.90 ($M^+ + 1$).Anal. calcd for $C_{10}H_9Cl_2NO_2S$: C, 43.18; H, 3.26; N, 5.04; S, 11.53%. Found: C, 43.14; H, 3.22; N, 5.02; S, 11.57%.

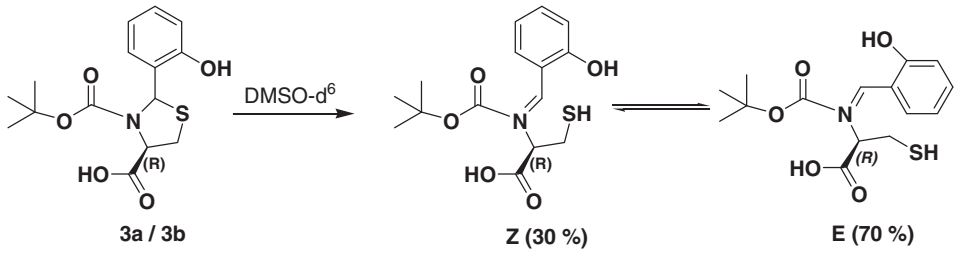

Figure 9. Conformational isomers obtained from **3a** and **3b** in DMSO-d_6.

5.19. (2S,4R)-3-(tert-butoxycarbonyl)-2-(2-hydroxyphenyl) thiazolidine-4-carboxylic acid (3a)

$C_{15}H_{19}NO_5S$, white solid, M.P 187°C (85%), $[\alpha]_D^{25}$ +10.7 (*c* 1.25, MeOH). IR(KBr): 3097(COOH), 1627 (C=O), 13,831,332, (C-S), 1280, 1238 (C-O), 1097, 1093, 761 (aromatic C-H) $cm^{-}1$, ^{1}H- NMR (DMSO-d_6): δ 10.3 (s, 1H,broad, H COOH), δ 7.83 (d, 1H, J = 8 Hz, H Ar), δ 7.17 (t, 1H, J = 8 Hz, H Ar), δ 6.83 (m, 2H, J = 8 Hz, H Ar), δ 5.93 (s, 1H, H-2), δ 4.86 (q, 1H, J = 7.2 Hz, H-4), δ, δ 3.43 (dd, 1H, J = 7.2, 4.5 Hz, H-5), δ 2.73 (dd, 1H, J = 7.2, 4.5 Hz, H-5), δ 1.38 (s, 6H, H $CH_3C(CH_3)_2$), δ 1.25 (s, 3H, H $CH_3C(CH_3)_2$). ^{13}C NMR (DMSO-d_6): 172.69 (C=O), 172.24 (C=O), 154.60, 130.29, 127.50, 120.47, 119.90, 115.13(C Ar), 83.35 (C $C(CH_3)_3$), 60.89 (C-2), 49.43 (C-4), (C-5, merged in DMSO-d_6 signals), 28.10 (C $C(CH_3)_3$). MS: 326.00 (M + 1)

5.20. (2R,4R)-3-(tert-butoxycarbonyl)-2-(2-hydroxyphenyl) thiazolidine-4-carboxylic acid (3b)

$C_{15}H_{19}NO_5S$, White solid, M.P 145°C; (15%). $[\alpha]_D^{25}$ +73.2 (*c* 1.25, MeOH).[25] IR (KBr,υ,cm^{-1}): 3389 (COOH), 1718 (C=O),1627, 1396 (C-S), 1282 (C-O), 908, 848 (aromatic C-H) cm^{-1}. ^{1}H NMR (DMSO-d_6): δ 9.66 (s, 1H, H COOH), δ 7.81 (d, 1H, J = 7.5 Hz, H Ar), 7.03 (m, J = 7.5, 1.5 Hz, 1H, H Ar), 6.73 (m, 2H, J = 7.5, 1.5 Hz, H Ar), 6.11 (s, 1H, H-2), 4.46 (dd, J = 7, 4.3 Hz, 1H, H-4), 3.37 (m, J = 7, 4.3 Hz, 1H, H-5), 3.07–2.90 (m, J = 7, 4.3 Hz, 1H, H-5), 1.32 (s, 6H, H $CH_3C(CH_3)_2$), δ 1.10 (s, 3H, H $CH_3C(CH_3)_2$). ^{13}C NMR (DMSO-d_6):172.20 (C=O), 171.82 (C=O), 153.58, 152.52, 127.97, 118.43, 114.50 (C Ar), 80.42 (C $C(CH_3)_3$), 64.60 (C-2), 61.06 (C-4), (C-5, merged in DMSO-d_6 signals), 27.65(C $C(CH_3)_3$). MS: 324.00 (M-1).

Though the X-ray data in the crystalline state compound **3a** have shown a trans-conformation, the doubling of signals of t-butyl group at 1.25 and 1.38 δ ppm, as well as the signals of Ar-OH at 10.25 and 10.37 δ ppm was found in the ^{1}H NMR spectrum of the compound **3a**. This splitting of the signals for t-butyl group can be attributed to the effect of the hindered rotation of the BOC-fragment relative to C-N bond (E-Z isomerism) in DMSO-d_6 represents the coexistence of a mixture of trans/cis isomers in the approximate ratio of trans/cis as 7/3. The same situation is observed for compound **3b**. This tendency of cis/trans isomerism in solutions is in accordance with a general property of N-acyl derivatives of thiazolidine-4-carboxylic acid [23] as shown in Figure 9.

Also, the melting point of compounds **3b** (145°C) is found to be in good agreement to its reported value (143–145°C).[41] However, compound **3a** showed higher melting point (187°C) than **3b**, which is attributed to more intermolecular attractive interactions of trans-oriented carboxylic acid group and 2-hydroxyphenyl ring substituent.

Acknowledgements

MAR thankfully acknowledges Dr Rahul Banerjee, CSIR-National Chemical Laboratory Pune, India for the X-ray crystallography.

Disclosure statement

No potential conflict of interest was reported by the author.

Funding

YD thanks CSIR-India for an SRF grant.

References

[1] Jin C, Burgess JP, Gopinathan MB, Brine GA. Chemical synthesis and structural elucidation of a new serotonin metabolite: (4R)-2-[(5′-hydroxy-1′*H*-indol-3′-yl)methyl]thiazolidine-4-carboxylic acid. Tetrahedron Lett. 2006;47:943–946.
[2] Lu Y, et al. Discovery of 4-substituted methoxybenzoyl-aryl-thiazole as novel anticancer agents: synthesis, biological evaluation, and structure—activity relationships. J Med Chem. 2009;52:1701–1711.
[3] Song Z, Ma GY, Lv PC, Li HQ, Xiao ZP, Zhu HL. Synthesis, structure and structure – activity relationship analysis of 3-*tert*-butoxycarbonyl-2-arylthiazolidine-4-carboxylic acid derivatives as potential antibacterial agents. Eur J Med Chem. 2009;44:3903–3908.
[4] Liu Y, et al. Design, synthesis and biological activity of thiazolidine-4-carboxylic acid derivatives as novel influenza neuraminidase inhibitors. Bioorg Med Chem. 2011;19:2342–2348.
[5] Onen-Bayram FE, Durmaz I, Scherman D, Herscovici J, Cetin-Atalay R. A novel thiazolidine compound induces caspase-9 dependent apoptosis in cancer cells. Bioorg Med Chem. 2012;20:5094–5102.
[6] Serra AC, et al. Synthesis of new 2-galactosylthiazolidine-4-carboxylic acid amides: antitumor evaluation against melanoma and breast cancer cells. Eur J Med Chem. 2012;53:398–402.
[7] Ohmae M, Koide S, Fujita Y, Kimura S. Enzymatic polymerization to an alternating N-l-cysteinyl chitin derivative: a novel class of multivalent glycopeptidomimetics. Carbohyd Res. 2013;377:28–34.
[8] Bertamino A, et al. Synthesis, in Vitro, and in cell studies of a new series of [Indoline-3,2′-thiazolidine]-based p53 modulators. J Med Chem. 2013;56:5407–5421.
[9] Pinhong C, et al. 2-Substituted 4,5-dihydrothiazole-4-carboxylic acids are novel inhibitors of metallo-β-lactamases. Bioorg Med Chem Lett. 2012;22:6229–6232.
[10] Lewis W, Steel PJ. Chiral heterocyclic ligands. XVI: Synthesis and crystal structures of four metal complexes of a tridentate, biheterocyclic ligand derived from l-cysteine. Polyhedron. 2010;29:2220–2224.
[11] Frimayanti N, Lee VS, Zain SM, Wahab HA, Rahman NA. 2D, 3D-QSAR, and pharmacophore studies on thiazolidine-4-carboxylic acid derivatives as neuraminidase inhibitors in H3N2 influenza virus. Med Chem Res. 2014;23:1447–1453.
[12] Katsuyama I, et al. Substituent-dependent reactivity in aldehyde transformations: 4-(phenylethynyl) benzaldehydes versus simple benzaldehydes. Tetrahedron. 2013;69:4098–4104.
[13] Schmolka IR, Spoerri PE. The preparation of 2-substituted thiazolidine-4-carboxylic acids 1,2. J Org Chem. 1957;22:943–946.

[14] Gyorgydeak Z, Kajtar-Peredy M, Kajtar J, Kajtar M. Synthese und chiroptische Eigenschaften von *N*-Acetyl-4-thiazolidincarbonsauren. Liebigs Ann Chem. 1987;1987:927–934.
[15] Markovic R, Rajkovic B. Synthesis of 2-aryl-substituted thiazolidine-4-carboxylic acids by intramolecular cycloaddition of *in situ* formed azomethine derivatives of L-cysteine. J Serb Chem Soc. 1997;62:957–964.
[16] Braga AL, Alves EF, Silveira CC, Zeni G, Appelt HR, Wessjohann LA. A new cysteine-derived ligand as catalyst for the addition odiethylzinc to aldehydes: the importance of a 'Free' sulfide site for enantioselectivity. Synthesis. 2005;2005:588–594.
[17] Saiz C, Wipf P, Manta E, Mahler G. Reversible thiazolidine exchange: a new reaction suitable for dynamic combinatorial chemistry. Org Lett. 2009;11:3170–3173.
[18] Ferraboschi P, et al. Synthesis of the new immunostimulating agent pidotimod (3-L-pyroglutamyl-L-thiazolidine-4-carboxylic acid) labelled with ^{14}C- and ^{35}S-isotopes. J Label Comp Rad. 1992;31:973–980.
[19] Wu C, Fu X, Li S. A highly efficient, large-scale, asymmetric direct aldol reaction employing simple threonine derivatives as recoverable organocatalysts in the presence of water. Eur J Org Chem. 2011;2011:1291–1299.
[20] Gong Z, et al. Novel chiral thiazoline-containing N-O ligands in the asymmetric addition of diethylzinc to aldehydes: substituent effect on the enantioselectivity. Appl Organomet Chem. 2012;26:121–129.
[21] Radomski J, Temeriusz A. Thiazolidine-4(*R*)-carboxylic acids derived from sugars: Part I, C-2-epimerisation in aqueous solutions. Carbohydr Res. 1989;187:223–237.
[22] Kumar M, et al. Synthesis of α,β-unsaturated δ-lactones by vinyl acetate mediated asymmetric cross-aldol reaction of acetaldehyde: mechanistic insights. Eur J Org Chem. 2014;2014:5247–5255.
[23] Szilagyi L, Gyorgydeak Z. Comments on the putative stereoselectivity in cysteine-aldehyde reactions, Selective C(2) inversion and C(4) epimerization in thiazolidine-4-carboxylic acids. J Am Chem Soc. 1979;101:427–432.
[24] Song ZC, Ma GY, Zhu HL. Synthesis, characterization and antibacterial activities of *N-tert*-butoxycarbonyl-thiazolidine carboxylic acid. RSC Adv. 2015;5:24824–24833.
[25] Ershov AY, Nasledov DG, Lagoda IV, Shamanin VV. Synthesis of 2-substituted (2*R*,4*R*)-3-(3-mercapto- propionyl) thiazolidine-4-carboxylic acids. Chem Heterocycl Compd. 2014;50: 1032–1038.
[26] Ershov AY, et al. Ring-chain tautomerism of 2-aryl-6-oxohexahydropyrimidine-4-carboxylic acid sodium salts. Chem Heterocycl Compd. 2013;49:598–603.
[27] Li T, Ayers PW, Liu S, Swadley MJ, Medendorp AC. Crystallization force-a density functional theory concept for revealing intermolecular interactions and molecular packing in organic crystals. Chem Eu J. 2009;15:361–371.
[28] Yanai T, Tew DP, Handy NC. A new hybrid exchange correlation functional using the Coulomb-attenuating method (CAM-B3LYP). Chem Phys Lett. 2004;393:51–57.
[29] Frank AJ, Otvos JW, Calvin M. Quenching of Rhodamine 101 emission in methanol and in colloidal suspensions of latex particles. J Phys Chem. 1979;83:716–722.
[30] Rizvi MA, et al. Nuclear blebbing of biologically active organoselenium compound towards human cervical cancer cell (HeLa): In vitro DNA/HSA binding, cleavage and cell imaging studies. Eur J Med Chem. 2015;90:876–888.
[31] Chrostowska A, et al. UV-Photoelectron spectroscopy of BN Indoles: experimental and computational electronic structure analysis. J Am Chem Soc. 2014;136:11813.
[32] Rusu E, Dorohoi DO, Airinei AJ. Solvatochromic effects in the absorption spectra of some azobenzene compounds. Mol Struct. 2008;887:216–219.
[33] Sharma S, Kumar M, Kumar V, Kumar N. Metal-free transfer hydrogenation of nitroarenes in water with vasicine: revelation of organocatalytic facet of an abundant alkaloid. J Org Chem. 2014;79:9433–9439.
[34] Fayet G, Rotureau P, Joubert L, Adamo C. On the prediction of thermal stability of nitroaromatic compounds using quantum chemical calculations. J Hazard Mater. 2009;171: 845–850.

[35] Kumar M, et al. Copper (II)-triflate-catalyzed oxidative amidation of terminal alkynes: a general approach to α-ketoamides. Asian J Org Chem. 2015;4:438–441.
[36] Fukui K, Yonezawa T, Shingu H. A perspectve orbital theory of reactivity in aromatic hydrobarbons. Theor ChemAcc. 2000;103:219–220.
[37] Issa RM, Awad MK, Atlam FM. Quantum chemical studies on the inhibition of corrosion of copper surface by substituted uracils. Appl Surf Sci. 2008;255:2433–2441.
[38] Parr RG, Pearson RG. Absolute hardness: companion parameter to absolute electronegativity. J Am Chem Soc. 1983;105:7512–7516.
[39] Pearson RG. Chemical Hardness: applications from molecules to solids. Weinheim: Wiley-VCH; 1997.
[40] Parr RG, Szentpaly LV, Liu S. Electrophilicity index. J Am Chem Soc. 1999;121:1922–1924.
[41] Benedini F, Ferrario F, Sala A, Sala L, Soresinetti PA. Synthesis and NMR studies of thiazolidine-4-carboxylic acid derivatives containing a nitro ester function. J Heterocyclic Chem. 1994;31:1343–1347.